

Utilizing GPS To Determine Ionospheric Delay Over the Ocean

*Stephen J. Katzberg and James L. Garrison, Jr.
Langley Research Center • Hampton, Virginia*

Available electronically at the following URL address: <http://techreports.larc.nasa.gov/ltrs/ltrs.html>

Printed copies available from the following:

NASA Center for AeroSpace Information
800 Elkridge Landing Road
Linthicum Heights, MD 21090-2934
(301) 621-0390

National Technical Information Service (NTIS)
5285 Port Royal Road
Springfield, VA 22161-2171
(703) 487-4650

Abstract

Several spaceborne altimeters have been built and flown, and others are being developed, to provide measurements of ocean and ice sheet topography. Until the launch of TOPEX, altimeters were single frequency systems incapable of removing the effects of ionospheric delay on the radar pulse. With the current state of the art in satellite altimetry, the ionosphere causes the largest single error when using single frequency altimeters. Ionospheric models provide the only recourse short of adding a second frequency to the altimeter. Unfortunately, measurements of the ionosphere are lacking over the oceans or ice sheets where they are most needed. A possible solution to the lack of data density may result from an expanded use of the Global Positioning System (GPS). This paper discusses how the reflection of the GPS signal from the ocean can be used to extend ionospheric measurements by simply adding a GPS receiver and downward-pointing antenna to satellites carrying single frequency altimeters. This paper presents results of a study assessing the feasibility and effectiveness of adding a GPS receiver and downward-pointing antenna to satellites carrying single frequency altimeters.

Introduction

Several spaceborne altimeters have been built and flown, and others are being developed, to provide measurements of ocean and ice sheet topography. Until the launch of TOPEX in 1992, altimeters were not capable of removing the effects of ionospheric delay on the radar pulse. Ionospheric delay can cause range errors of tens of centimeters at the high frequencies employed by satellite altimeters. TOPEX addressed the problem of ionospheric delay by using the frequency dependence of the ionospheric delay and two sufficiently separated altimeter frequencies. TOPEX requires two altimeters integrated as much as possible into the same spacecraft with the attendant cost, complexity, and extra failure modes.

Nevertheless, single frequency altimeters are considered useful for certain applications and continue to be built. For short arc topography or low ionospheric total electron concentration, ionospheric errors may not be important. For global ocean circulation modelling, in which the ionosphere represents the largest single error, ionospheric altimeter models are relied upon to provide necessary corrections. Current models are accurate and yield corrections which, prior to TOPEX, were considered adequate. The TOPEX performance in altimeter accuracy, precision orbit determination, water vapor corrections, and stability has increased performance expectations considerably. Whereas in 1992 an ionospheric model capable of a 5-cm root-mean-square accuracy at any selected orbit point would not appreciably affect the end-to-end measurement accuracy, such a measurement today would degrade performance by nearly 50 percent based on TOPEX published data.

The best ionospheric models are accurate over fairly short arcs and only when supplied with actual measurements of the ionosphere. These models are competitive

with TOPEX dual frequency ionospheric measurements only when there is a high density of data samples. Unfortunately, measurements of the ionosphere are lacking over the oceans or ice sheets where they are needed most.

A possible solution to the lack of data density may come from an alternative use of the Global Positioning System (GPS). This paper proposes that because the GPS satellite system floods the Earth with radiant energy, the reflection of the GPS signal from the ocean can be used to extend ionospheric measurements by adding a GPS receiver and downward-pointing antenna to any satellite carrying a single frequency altimeter. Experimental evidence that scattering of GPS signals from the ocean can be detected has been presented by Auber, Bibaut, and Rigal (ref. 1). The present paper presents results of a study assessing feasibility and effectiveness of using scattered GPS signals.

Following results of work by Beckmann and Spizichino (ref. 2), the characteristics of the GPS signal bouncing from the ocean are presented and then extended. An analysis of the following reflected signal characteristics is given: power, signal density versus delay, relationship to the direct signal, the specular component, and the diffuse component. Expected effects in the receiver and the degree to which the ionospheric delay can be tracked are discussed. Finally, the degree to which this technique can be used to supplement a single frequency altimeter both directly and with ionospheric models is presented.

In the succeeding discussion, reference is made to various aspects of the GPS with the assumption that the reader is aware of general technical details related to the GPS. More information on the GPS can be found in publications such as reference 3.

Symbols

A	scattering area, m^2	β	angle formed between local surface normal and vector difference of GPS propagation vector and scattering vector to altimeter satellite
A_a	antenna effective area, m^2	β_0	equivalent slope angle of surface irregularities
a, b	semimajor and semiminor axes for locus of points with fixed delay	γ	grazing angle, deg or rad
a, b, c	geometric factors in appendix A from reference 2	δ	path length difference, m
C/A	coarse acquisition, a mode of low resolution for GPS	ζ	surface topography in z direction, m
c	speed of light, m/sec	θ, θ_i	spherical coordinates
F	geometric scattering factor	Λ	triangle function
f	frequency, Hz	λ	wavelength, m
G	Green's function	ρ	reflectance
GPS	Global Positioning System	σ_0	differential backscattering coefficient
H	size of vertical irregularities, m	τ, τ_{code}	time interval or time duration of one C/A chip, sec
h	satellite altitude, m	ω	radian frequency, Hz
k	propagation constant, 1/m	'	denotes partial derivative with respect to x or y as appropriate
L	linear dimension of illuminated area, m		
LHCP	left-hand circularly polarized		
P	any point on surface		
P_a, P_t	power received at altimeter satellite and GPS transmitted power, respectively, W		
PRN	pseudorandom noise, acronym for any specific C/A code transmitted by GPS satellite		
R	reflectance		
RHCP	right-hand circularly polarized		
R_a, R_0	range from satellite to scattering surface, m		
r	radius		
r_s, r_a	distances from surface to altimeter satellite and GPS satellite, respectively		
dS	differential surface area, m^2		
TEC	total electron concentration, 1×10^{16} electrons/ m^2		
t	time, sec		
u, v	azimuthal angle and angle with respect to x, y plane of scattering angle to satellite, respectively		
v_x, v_z	x - and z - components of propagation vector		
X, Y	lateral extent of scattering integral areas, m		
X_0	ellipse center, specular point of ocean surface		
x, y	surface coordinates		
Y	received signal correlation function		
z	axis normal to local ocean surface		

Ionospheric Models and Total Electron Concentration

The primary difficulty for altimeters caused by the ionosphere is the propagation delay caused by free electrons. The group delay for an altimeter pulse travelling through the ionosphere is typically expressed by

$$dx = 40.5 \left(\frac{1}{f^2} \right) \text{TEC} \quad (1)$$

where dx is in centimeters, f is in gigahertz, and TEC is 10^{16} electrons/ m^2 and represents total column density of ionospheric electrons. Maximum values for total electron concentration are about 100 TEC units, which yields a path length error at 13.7 GHz (TOPEX and GEOSAT altimeter frequencies) of about 20 cm. Present determination of exact repeat orbits within very few centimeters in radial error, altimeters capable of about a centimeter of pure range accuracy, and water vapor correction factors in the centimeter range show that single frequency altimeter accuracy is dominated by ionospheric error. In addition, various features of the ionosphere such as the South Atlantic anomaly (ref. 4) have spatial characteristics that could be mistaken for ocean surface topographic features.

The only recourse other than a second altimeter frequency is the use of ionospheric models capable of utilizing actual measured data. The only known model with the capability of ingesting measured data and improving accuracy is the Parameterized Real-Time Ionosphere Model (PRISM) developed by U.S. Air Force. Studies

utilizing TOPEX ionospheric data to determine the effectiveness of PRISM in predicting total electron concentration suggest that the ionosphere spatially decorrelates over distances greater than approximately 500 km. Stated more directly, PRISM shows no improvement with ionospheric data ingested at distances greater than a few hundred kilometers, and at greater distances errors can actually increase after "correction."

The more direct Global Ionosphere Map (GIM) developed by Jet Propulsion Laboratory (JPL) is based on GPS data in direct transmission. When augmented by TOPEX data to gain a temporary extension of the data over global regions without ground stations, GIM performs equally with the more complex PRISM approach. Thus, one profitable method to realize the greatest return from single frequency altimeters might be to extend the ionospheric sampling as far as possible over the oceans and ice caps.

GPS-Based Ionospheric Correction Technique

Given the desire to extend the spatial sampling of real ionospheric data into otherwise inaccessible global regions, or better, to get information from available sources coincident with the satellite carrying the single frequency altimeter, several possibilities have been suggested. These include ionosondes carried on spacecraft separately or integrated with the altimeter satellite and tomography utilizing either dual frequency beacons or the dual frequencies inherent in the GPS signal. This paper focuses on an alternative to previously suggested uses of GPS signals for ionospheric sampling.

The measurement technique presented in this section starts with understanding that the GPS satellite constellation illuminates the Earth's surface with a low-level radio frequency (RF) field of well-known characteristics. It follows that the signal from the GPS satellite strikes both the ice caps and all oceans. If the oceans are mirrorlike, then the signal bounced from the ocean to an observing satellite follows a path only slightly longer than a direct-to-satellite path. However, the signal from the Earth's surface would experience an oblique, double pass through the Earth's atmosphere, including the ionosphere. While the accuracy of all but the phase tracking signals of GPS satellites is far coarser than the range accuracy for an altimeter, the GPS signal enjoys a leverage effect derived from equation (1). The frequencies of GPS signals are approximately an order of magnitude lower than the 13.7-GHz signal and consequently a given TEC will cause a delay in the GPS signal of the frequency ratio squared (approximately a factor of 100). Thus, a 100 TEC 20-cm delay for the altimeter at 13.7 GHz will appear as a 20-m delay at the 1.575-GHz (L1 band) frequency for the GPS. In addition, the

oblique path and double pass will at least double this delay to more than 40 m.

Because GPS satellites are at a range of approximately 26 000 km from Earth center, the double pass off the Earth's surface will constitute an increase in path length of more than twice the satellite orbital altitude. For typical altimeter satellites, this additional distance will be about 2000 km. When the entire path distance is considered, the possible loss in power would only be on the order of 2 percent. At the ocean bounce, there would be a loss of signal from the reflectance of seawater or ice.

The GPS satellite signal would then be received by an antenna placed on the underside of the altimeter satellite and fed to the RF amplifier and detection and processing electronics in the GPS receiver. In this simple scenario the reflected signal is specular and is detected in the same fashion as the normal signal is detected. The only difference is the unexpected delay determined in the code-phase-lock circuitry. Included in this measured delay would be the geometric path delay and the ionospheric delay over the slant path taken. If, as sometimes given as a rule of thumb for GPS pseudorange determination, the C/A code can be determined to 1/100 chip over 1 sec averaging, then it should be possible to determine the ionospheric delay to a similar accuracy (approximately 3 m). The 40-m ionosphere-induced range error would be determinable to approximately 1/10 its value. The 20-cm range error at 13.7 GHz would be reduced to 2 cm with 1 sec averaging.

This oversimplified proposition glosses over several factors, and several questions must be answered before credibility can be established. Is the GPS signal structure modified by reflection from the ocean? Is the polarization of the signal changed at the ocean interface and if so, what losses are incurred? What are the effects of the slant path when sampling is not done directly under the spacecraft? After the signal reaches the spacecraft, is there sufficient signal-to-noise ratio available to yield useful ionospheric measurements? Can the possibly modified signal be processed effectively, and if so, under what constraints? This paper addresses these questions and establishes the conditions and hardware and software modifications that will allow this GPS-based approach to work.

Modelling Ocean Bounce Signal

Scattering of GPS Signal

To understand what happens when a GPS signal hits the ocean, note that there are two (not necessarily exclusive) classes of radiation emanating from the ocean surface. One class of radiation is purely specular and the effect is mirrorlike, retaining phase coherence. The other

class of radiation is diffuse, and the coherence is lost and radiation exists from angles other than the specular direction. As the flatness and lateral extent of the features (waves, ripples, and so forth) on the scattering surface decrease, the reflected RF field is expected to change from predominantly specular to exclusively diffuse in character. Diffuse conditions arise because the surface becomes increasingly composed of high-slope short-range facets that reflect the GPS radio field into widely distributed angles.

An historical rule of thumb used to mark the onset of diffuse scattering is the Rayleigh criterion which can be expressed as

$$\lambda > 8H \sin \gamma \quad (2)$$

where H is the size of the vertical irregularities, γ is the angle with respect to the horizontal surface with which the irregularities are viewed, and λ is the (monochromatic) radiation wavelength. In effect, if the projected surface roughness exceeds $\pi/2$, then the propagated phase will be sufficiently modified to cause significant reduction of the far-field pattern in the specular direction. For GPS wavelengths of L1 band frequency (1.57542 GHz, 19 cm) and L2 band frequency (1.22760 GHz, 24 cm), typical ocean wave heights and structure would exceed these (L1 and L2 band) modest wavelengths and be well into the Rayleigh-defined onset of diffuse scattering (ref. 1). Consequently, Auber, Bibaut, and Rigal (ref. 1) were somewhat surprised when they found their GPS receiver locking onto the signal reflected off the water. Experimental literature would not have been helpful in anticipating this result.

Typical applications of radar utilize a monostatic measurement in which the radar transmitter and receiver are integrated. Therefore, measurements of radar return are of backscatter, and while the literature is full of data on backscatter measurements, the data are of little use for evaluating ocean reflectance. For ocean reflectance, the bounce from the ocean is akin to a bistatic configuration and is more appropriate to radio transmitter-receiver links over land and water than radar. Moreover, the frequency ranges used are almost exclusively very much higher than the GPS signals.

Auber, Bibaut, and Rigal (ref. 1) explained their results by applying diffuse scattering models developed by Beckmann and Spizzichino (ref. 2). To extend the results of Auber, Bibaut, and Rigal (ref. 1) examining the satellite altitude by using models developed in reference 2 is helpful.

Figure 1 illustrates the geometry for an altimeter satellite less than a couple thousand kilometers above the Earth compared with GPS constellation orbit altitudes.

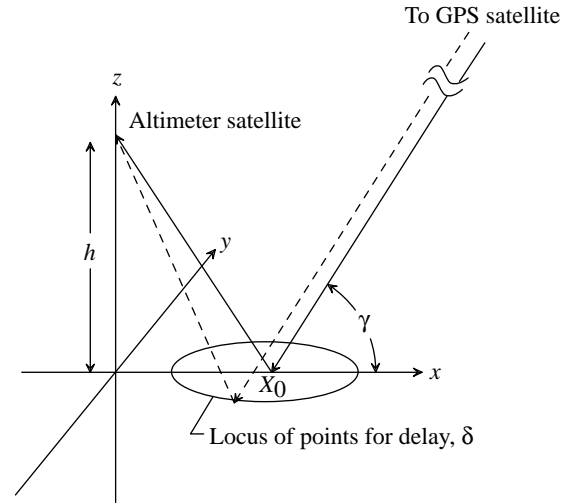


Figure 1. Illustration of scattering geometry from GPS satellite to altimeter satellite.

The GPS satellite is assumed very far (tens of thousands of kilometers) away compared with the altimeter satellite. To model the desired effects of terrestrial bounce, two path-length differences are necessary: (1) the difference between the direct-from-GPS path and the ocean-bounce-to-altimeter path and (2) the difference between the path from the specular point on the ocean surface and any other path from the ocean surface to the altimeter satellite. For simplicity a locally flat Earth is assumed, which is a good assumption for determining Fresnel zones in which path lengths differ from zone to zone by a half wavelength out of thousands of kilometers. The cases in this report involve a satellite altimeter much closer to the Earth than the GPS satellites, and the locally flat Earth can be assumed normal to the Earth-center altimeter-satellite line. The specular point represents the shortest distance from GPS satellite to altimeter satellite for both the flat Earth case and the real case. The correct location on the Earth for the specular point is different in the two cases but is easily calculated.

The previous considerations lead to the reason for the importance of referring the signal path lengths to the specular point. All bounce signals from the GPS satellite can come no earlier than the signal from the specular point. Code correlators in the GPS receivers are assumed linear, and in determining pseudorange the processors report a distribution of delays at least as long as the delay from the specular point. The distribution of delays is longer than the delay corresponding to the direct path (within the code phase ambiguity interval, or modulo 300 km for C/A code).

When applying the assumptions in the previous paragraphs, the specular point will occur at a distance $h \cot \gamma$

from the subsatellite point. The range of δ with respect to the direct-from-GPS path is

$$\delta = 2h \sin \gamma \quad (3)$$

This range difference reaches a maximum value of $2h$ when the GPS satellite is directly above the altimeter satellite. This distance will always be greater than the C/A code ambiguity range of 300 km (1023 chips), and interpretation of data must take this into account.

Figure 1 illustrates the locus of points corresponding to a fixed delay and is an ellipse that is expressed as (ref. 2)

$$\delta = \sqrt{x^2 + y^2 + h^2} - x \cos \gamma - h \sin \gamma \quad (4)$$

Equation (4) can be used to express the Fresnel zones by setting δ equal to $\lambda/2$. For the case addressed here, δ is much larger and represents fractions of C/A code chips (300 m).

The semimajor and semiminor axes of the ellipse corresponding to one chip (300 m) are given, respectively, by

$$a = \sqrt{\frac{2\delta h \sin \gamma}{\sin^2 \gamma}} \quad (5a)$$

and

$$b = \sqrt{\frac{2\delta h \sin \gamma}{\sin \gamma}} \quad (5b)$$

where the small quadratic term in the delay is ignored compared with the height h of the altimeter satellite. Finally, the location of the center of the ellipse is derived from

$$h = X_0 \tan \gamma - \frac{\delta}{\sin \gamma} \quad (6)$$

Since this fact is used later, note that the ellipse interior represents the total area contributing to a signal with delay less than or equal to δ .

Diffuse Scattering From Surface

Unfortunately, the surface of the ocean or land is dominated by the diffuse component of the reflected signal. Reference 2 provides a complete development of a scattering model based on the assumption of stationary, randomly distributed surface heights with random but stationary spatial correlations. This scattering model results in an angularly dependent scattering cross section that can be expressed as the standard deviation of the surface height features and their correlation distance. The scattering model yields an extension of the Rayleigh cri-

terion and allows more flexibility in defining the onset of diffuse scattering.

The scattering model predicts that the scattering cross section under rough ocean or land surface conditions should be

$$\sigma_0(\beta) = \cot^2 \beta_0 \exp\left(-\frac{\tan^2 \beta}{\tan^2 \beta_0}\right) \quad (7)$$

This scattering model assumes Gaussian-distributed surface heights and a correlation function for these heights which varies exponentially with an argument of negative quadratic variation with distance between points. The characteristic distance is T , such that at T separation the height correlation is down to $1/e$. The term $\tan \beta_0$ (eq. (7)) is the ratio of twice the standard deviation of the height divided by the correlation distance T . The term $\tan \beta_0$ may be thought of as representing an average slope of the surface irregularities. The angle β (fig. 2) is an angle defined in steps as (1) construct the vector bisector of the incident RF propagation vector and the scattering vector and (2) the angle β is the angle between the local surface normal (the z -axis in this case) and the vector bisector.

This model predicts that with smaller β_0 , more scattering is concentrated along the specular direction. Along the specular direction the cross section is maximum and decreases rapidly away from the specular direction. In addition, a "glistening surface" may be defined which represents the area on the ocean surface in which $\beta = \beta_0$. Within this area the cross section is approximately $\cot^2 \beta_0$. As seen later, the code correlation reflectance area is inside the glistening surface, but

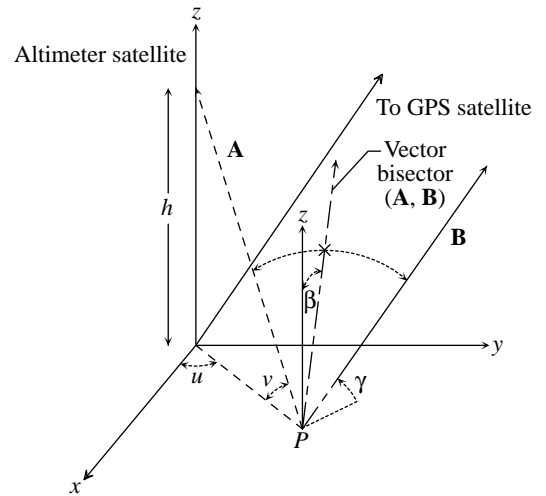


Figure 2. Illustration of scattering geometry defining bisector angle β .

always remember there is a maximum area from which significant scatter can occur. In compensation, the small β_0 case is one that approaches the specular limit. The model must be changed from assuming a very rough ocean surface to assuming a slightly rough ocean surface with a concomitant increase in the scattered power in the desired direction, improving rather than diminishing the prospects for effective receiver performance.

Glistening Surface

Before calculating the ocean return signal, determining the size of the glistening surface is necessary. Since the glistening surface is set by the dispersion of the ocean scattering angles and the code phase reflecting area is set by the size of the particular time delay interval, it is possible that the glistening surface can overlap or underfill the code phase reflecting surface.

The glistening surface is approximately centered near the specular point for vanishingly small β_0 . As noted, the specular point is also the point of minimum range difference from GPS to altimeter satellite via the ocean. Therefore, the code phase reflectance region and the glistening surface are both centered around the specular point. As will be seen, the glistening surface and the code phase reflecting surfaces are both circles for large grazing angle and near specular scattering. However, as the scattering angle becomes larger the glistening surface is no longer circular and takes on an elliptical character. The code phase reflecting area becomes very elliptical; the two figures differ considerably and calculations are required. By modelling the various vectors from GPS to ocean and from ocean to altimeter satellite and the unit vector that bisects the two others, the cosine of bisector-angle to the vertical axis is solved by the following equation (ref. 2):

$$2 \cos u = \frac{\cos \gamma}{\cos v} + \frac{\cos v}{\cos \gamma} - \tan^2 \beta_0 \frac{(\sin \gamma + \sin v)^2}{\cos \gamma \cos v} \quad (8)$$

Rewriting the above equation in terms of the x' , y' , z' axes makes it possible to express equation (8) as follows:

$$\frac{2x}{(h^2 + x^2 + y^2)^{1/2}} = \cos \gamma + \frac{x^2 + y^2}{\cos \gamma (h^2 + x^2 + y^2)} - \tan^2 \beta_0 \times \frac{[\sin \gamma + h/(h^2 + x^2 + y^2)^{1/2}]}{\cos \gamma} \quad (9)$$

If the subsatellite ionosphere is of most interest, γ can be assumed to be large (approaching 90°) and h can be

assumed to be larger than either x or y or their root sum-squares; this equation can thus be simplified to

$$(x - h \cos \gamma)^2 + y^2 = h^2 \tan^2 \beta_0 (\sin \gamma + 1)^2 \quad (10)$$

which is the equation of a circle with a center at the specular point. (Note that $h \cos \gamma$ is the approximate value for $\cot \gamma$, since $\sin \gamma$ is assumed to be near unity.)

An expansion of equation (9) shows that the glistening surface is bounded by a figure symmetric with respect to y but unsymmetrical to any point on x , except in the limit given here; however, the figure is centered around the specular point (elongated in x) and collapses to the specular point when β_0 approaches zero.

Polarization Effects

The effect of the reflection on the polarization of the GPS signal must also be considered. The transmitted GPS signal is right-hand circularly polarized (RHCP) and an interaction with a partially conducting, dielectric surface is expected to modify the polarization. Moreover, GPS antennas are generally chosen to respond best to right-hand circularly polarized fields, therefore the surface reflection can affect the type of antenna that must be used.

The difference between horizontal and vertical polarization reflectances from the ocean is most pronounced near a grazing angle of 5° (for 20 cm wavelength) but changes to virtually identical values (as it should) at high angles (ref. 2). At low angles a considerable shift occurs in the relative reflectiveness, and results in near linear polarization. At the higher angles the polarization is gradually changed to left-hand circularly polarized (LHCP) component. Figure 3 summarizes the value of the polarization components (power in the RHCP and LHCP components) as a function of grazing angle. The small effects of loss due to penetration of the conducting sea surface are ignored.

In the scattering model (ref. 2) the surface is considered composed of randomly distributed slopes. For slopes whose extent represents several wavelengths and for higher grazing angles, it is reasonable to assume that the GPS RF field scattered from the ocean surface is all left-hand circularly polarized. For lower grazing angles and for scattering away from the specular direction, significant right-hand circular polarization is expected to remain after reflection.

Received Signal

Now that all required effects on GPS signals bounced from the ocean have been identified and collected, we can determine (1) if there is enough signal for

detection and (2) under what conditions the signal is useful for determining ionospheric correction.

To determine if enough signal is available for detection, assume that the code phase processing in the GPS receiver will need signal power similar to the power from the direct signal and simultaneously correspond to a delay within a code correlation chip. The power received at the antenna terminals can be written as the GPS-transmitted power density multiplied by differential area within the area of interest on the ocean surface. This power is multiplied by the scattering cross section evaluated at the scattering angle to the altimeter satellite, divided by the distance to the altimeter satellite squared, and integrated over the desired area as follows:

$$P_a = \int dS \frac{P_t \sigma_0 A_a}{4\pi R_a^2} \quad (11)$$

From equation (5) the semimajor and semiminor axes of the ellipse corresponding to one 300-m chip are, respectively,

$$a = \sqrt{\frac{2hc\tau \sin \gamma}{\sin^2 \gamma}} \quad (12a)$$

and

$$b = \sqrt{\frac{2hc\tau}{\sin \gamma}} \quad (12b)$$

and the difference in area between two successive chips is

$$A = \frac{2\pi hc\tau}{\sin^2 \gamma} \quad (13)$$

Equation (13) follows because the eccentricity of the ellipse is constant and the difference in areas is directly proportional to the chip length and satellite height.

Since the conditions selected for this analysis correspond to the first few chips of delay and are near the specular point, the variation of range to the altimeter satellite is very small. Therefore, the range can be removed from the integral. Similarly, the glistening surface is defined to provide a constant cross section, $\cot^2 \beta_0$ inside its boundary, and the variation of angle is small across the one-chip area. Therefore, the glistening surface is considered to have a constant effect until its boundary is reached. This boundary, as discussed previously, is nearly circular about the specular point, and hence is concentric with the code chip annuli (locus of points for

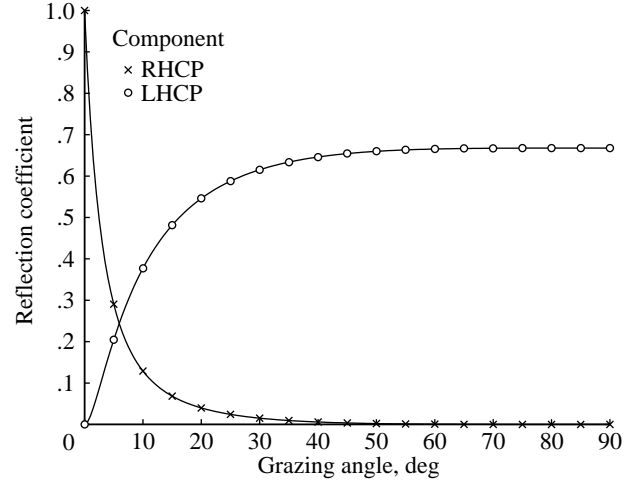


Figure 3. Resolution of reflected signal into left-hand and right-hand circularly polarized components.

constant code chip range delay). The integral is then the area corresponding to any two values of δ multiplied by the factors in range, reflectance, antenna area, incident power, and cross section as follows:

$$P_a = \frac{hc\tau_{\text{code}}}{2\sin^2 \gamma R_a^2} \sigma_0 A_a \quad (14)$$

The factor A_a (eq. (14)) represents the effective area of the antenna on the altimeter satellite and is assumed to be the same for the required top antenna receiving the direct GPS signal. The value for β_0 depends on the scattering angular extent and is equal to $\cot^2 \beta_0$ (ref. 2). The ratio of signal power from the ocean versus direct-to-satellite signal power is captured in the first factor in equation (14) and β_0 . Note also that $h/\sin \gamma$ is the same as R_a , canceling out one such factor. As examples, the reduction in GPS signal power for a satellite at 400 km would be 0.0047 (one chip average) whereas the reduction in signal at 800 km would be 0.0024 (one chip average). These values are then compensated by the scattering cross section $\cot^2 \beta_0$, requiring scattering angles of 3.0° (800 km) and 4.0° (400 km) to have signal power in one chip on the order of that in the direct-to-antenna power.

At first it seems unlikely that the bounce signal would be as powerful as the direct signal. However, as noted previously the ocean is highly reflective, and the distribution of delays within one chip is only over an annulus on the ocean surface well within the receiver antenna pattern.

Effect on Code Correlation

The signal reflected from the ocean consists of the transmitted GPS signal delayed over a wide range of times greater than or equal to the delay from the specular point. When the particular PRN code corresponding to the particular GPS satellite (PRN_{ref}) is cross-correlated with the received signal (PRN_{tm}), the following output is obtained:

$$Y(\tau) = \int \text{PRN}_{\text{ref}}(t + t_{\text{off}} - \tau) X(t) dt \quad (15)$$

where $X(t)$ is expressed by

$$X(t) = \int \text{PRN}_{\text{tm}}\left(t - T_{\text{as}} - \frac{\delta}{c}\right) \sqrt{P_t} R(r_s) G(r_a, r_s) d^2 r_s \quad (16)$$

Assuming that the code correlation process is effected in a time short enough for the surface integration to be constant allows the integration to be performed in equation (15) as follows:

$$Y(\tau) = \int \Lambda\left(T_{\text{as}} + \frac{\delta}{c} + t_{\text{off}} - \tau\right) \sqrt{P_t} R(r_s) G(r_a, r_s) d^2 r_s \quad (17)$$

where $\int \text{PRN}(t + \tau) \text{PRN}(t) dt$ has been replaced by the Λ function. In equation (17) T_{as} is the bulk delay from the GPS satellite through the specular point on the ocean surface and on to the altimeter satellite and t_{off} represents the difference between the GPS satellite clock and the receiver clock. The factor $R(r_s) G(r_a, r_s)$ represents the received field strength at the altimeter satellite (assuming incident power density P_t on the ocean) and combines all geometric effects given in the link analysis as a function of path delay δ , which is the excess over that of the specular point.

Two limiting cases must be considered before proceeding. In one case ocean scattering is specular, and in the other case ocean scattering is diffuse. For specular scattering the effect is the same as if the GPS satellite was shifted to lie along a line from the altimeter satellite to the specular point. The distance along that line would be the same as the distance from the GPS satellite to the specular point at its actual location. This case is a mirror reflection of the GPS satellite about the ocean surface. Since the increased distance to the altimeter satellite has a small effect on the received field strength or power, this case is the same as that for the direct path to the altimeter satellite. The only difference is the polarization modification and slight reflection loss at the ocean surface. Any ability to determine added delay from the ionosphere would be identical to this previously demonstrated capability of GPS receivers.

Diffuse scattering represents a more difficult situation. The phase coherence of the bounce signal is assumed lost because of the scattering from the variable topography of the ocean. Reference 2 details diffuse reflection from the ocean in which the authors select a normally distributed surface topography as the basis of their model and analysis. This case is the same as the case presented in reference 2 except for the fact that the reference 2 starting point (equation (3) of chapter 3, section 3.1) of

$$E = \exp(i\omega t - ik \cdot r)$$

must be modified. The exponential time dependence assumed for the incoming plane wave must be augmented by assuming that the exponential time dependence of the wave at any point is modulated by the PRN (biphase) code. The remaining information in reference 2 is then applicable with certain reservations. Because the PRN modulation signal bandwidth is narrowband compared with the L1 carrier frequency, the information in reference 2 (which, as noted, assumes a single frequency) need not be modified. The variation in propagation constant over the small frequency range involved in the modulation components does not change the Helmholtz integral and Fraunhofer far-field calculation for the spatial extent of interest here. Time variability reappears as a concern, since the field reflected from some area on the ocean undergoes a time variation from the rapid motion of the satellite along its ground track. New areas of ocean will have different scattering slopes and these will overlay the PRN modulation.

Stated differently, each scattering area on the ocean surface will contribute some specific delayed component of the PRN depending on its relative range. As long as a specific small range of time delay arises from the same scattering surface for the bulk of one C/A code phase repeat cycle (1 msec) the PRN modulation can be inverted. If not, the inversion efficiency will decrease, leaving only noise.

The altimeter satellite will be moving near 6 km/sec or more ground track speed, so 1 msec corresponds to 0.6 km. Fortunately, the ocean surface size of one C/A code chip, using equation (5b) with δ 300 m, will be approximately

15.5 km in radius for a satellite at 800 km and $\gamma \approx 90^\circ$. The possible change in viewed area will therefore be very small. Nonetheless, the detected signal after cross-correlation will still be a noise-like signal convolved with the triangular PRN autocorrelation function. Moreover, after squaring and filtering the signal will, over the time intervals required for smoothing, be subject to the full effect of the noise in the fluctuating return from the ocean. Any individual, sufficiently small reflecting area on the surface will scatter a replica of the PRN, with no particular carrier phase relationship to other areas.

It is convenient to approximate this scattering effect as if the reflected signal is uncorrelated except through auto-correlation from identical points. Thus, when the collected signal is multiplied by its particular PRN then squared and filtered, the result can be thought of as generating a short-time average proportional to the reflected power as follows:

$$\begin{aligned} \langle Y^2(\tau, t) \rangle &= \left\langle \frac{1}{T} \int_{t-T/2}^{t+T/2} Y(\tau, t') Y(\tau, t') dt' \right\rangle \\ &= \iint \Lambda^2 \left(\tau - T_{as} - \frac{\delta}{c} - t_{\text{off}} \right) P_t(r_s) \langle R(r'_s) R(r_s) G(r_s, r_a) G(r'_s, r_a) \rangle d^2 r_s d^2 r'_s \end{aligned} \quad (18)$$

Assuming correlation only from scattering points close to the same value of δ , the short-time average yields

$$\langle Y^2(\tau) \rangle = \Lambda^2 \left(\tau - T_{as} - \frac{\delta}{c} - t_{\text{off}} \right) P_t(r_s) \iint \langle R(r'_s) R(r_s) G(r_s, r_a) G(r'_s, r_a) \rangle d^2 r_s d^2 r'_s \quad (19)$$

The appendix shows how the double integral and internal expectation now take on the role of the variance of the reflectance and Green's function (ref. 2), resulting in the scattering cross section, glistening surface, and other related results detailed in reference 2.

The expectation of y^2 is now recognized as the power per unit area at locations corresponding to a particular delay δ of the scattered signal. The total power corresponding to delay δ being received is then the differential surface area between δ and $\delta + \Delta\delta$ times this power per unit area.

Since the surface area is expressible as a linear function of δ , the received (squared and filtered) signal is found by integrating the delayed lambda function over the surface area corresponding to the delay. From equation (19) the integral can be recognized as the convolution of the lambda function with the surface area integral evaluated at the appropriate delay δ as follows:

$$\int \langle Y^2(\tau) \rangle \frac{dA}{d\delta} d\delta = \int \langle Y^2(\tau) \rangle d^2 r \quad (20a)$$

$$\begin{aligned} \int \langle Y^2(\tau) \rangle \frac{dA}{d\delta} d\delta &= \int \underbrace{\Lambda^2 \left(\tau - T_{as} - \frac{\delta}{c} - t_{\text{off}} \right) P_t(r_s)}_{(1)} \\ &\quad \times \underbrace{\iint \langle R(r'_s) R(r_s) G(r_s, r_a) G(r'_s, r_a) \rangle d^2 r_s d^2 r'_s}_{(2)} \underbrace{\frac{2\pi h}{\sin^2 \gamma} d\delta}_{(3)} \end{aligned} \quad (20b)$$

$$\begin{aligned} \int \langle Y^2(\tau) \rangle \frac{dA}{d\delta} d\delta &= \int \frac{A^2 \cos^2 \theta_1}{\lambda^2 R_0^2} F_3^2 \lambda^2 \cot^2 \beta_0 \frac{\exp(-\tan^2 \beta / \tan^2 \beta_0)}{A \pi (\cos \theta_1 \cos \theta_2)^2} \\ &\quad \times \Lambda^2 \left(\tau - T_{as} - \frac{\delta}{c} - t_{\text{off}} \right) \frac{2\pi h}{\sin^2 \gamma} d\delta \end{aligned} \quad (20c)$$

where the expression for differential area (factor (3), eq. (20b)) has been introduced from equation (14) with $c\tau_{\text{code}}$ identified as δ , the excess delay from the specular point. Factor (2) (eq. (20b)) can be identified with the differential mean

square reflectance of section 12.4.1, equation (7) in reference 2. The equation is scaled by the actual surface RF power P_t .

The evaluation of equations (20) can be effected by noticing several factors. First, over the sizes of chips or fractions of chips of interest in this report, the range factors in equation (20) can be taken out of the integral, since chips correspond to annuli of a few kilometers in diameter while the satellite distance is hundreds of kilometers. Second, the integral represents the scattered signal over some differential area. This differential area can be calculated with a particularly convenient geometry by using the area between two successive ellipses (separated by $d\delta$ distance) with each ellipse representing the locus of points on the surface at a fixed δ (or δ and $\delta + d\delta$, in this case). Using the assumptions in this report relating to the glistening surface, the rest of the integral is constant. Finally, the outer limit of the integral is the ellipse (or more accurately, a circle) corresponding to the extent (where $\beta = \beta_0$) of the glistening surface.

Therefore, the received signal power is directly proportional to a quadratic function of the delay, with the proportionality constants being the cross section, the inverse of range, and the incident power density. The proportionality factors must not be so severe as to significantly reduce the signal below what occurs in the direct-from-GPS path. Furthermore, the glistening surface must not extend greater than a few chips, preferably less. The more the glistening surface is confined, the more the power density increases automatically. Better still, the range of δ between its zero value (relative to the specular point) and the glistening surface boundary sets the range of values of δ that will provide correlations. Knowing this simple result allows the determination of how the code phase error circuitry will behave in the presence of the distribution of time delays emanating from the ocean surface.

For example, if the glistening surface corresponds to 6° it will be approximately 40 km in radius for a satellite at 400 km. But one chip represents about 12.5 km, and the code phase correlation will be spread over nearly three (300 m) code chips to 900 m. Since the ionospheric error will be on the order of 40 m, it will take considerable filtering to accurately determine the glistening surface. For the cases mentioned in this report in which the cross section was small enough to balance out the range losses, the glistening surface is approximately one third of 6° . The correlation dispersion then corresponds to 300 m or less. Filtering requirements would be significantly relaxed.

Concluding Remarks

To summarize, if ocean reflectance can be represented as specular or nearly specular, then the bounced GPS signal received at satellite altitude is nearly as strong as the direct signal. The ability to detect the ionospheric delay is limited only by the inherent accuracy of the C/A range accuracy which is about one hundredth of a chip (3 m). This accuracy represents about one tenth the value of a typical high value ionospheric range error. The typical ionospheric delay value used in this report is 40 m (at 1.5 GHz) and corresponds to 20 cm at 13.7 GHz. Thus, it is possible to determine the ionospheric delay to better than 2 cm.

The required degree of specularity can be further clarified by noting that as long as the glistening surface is contained within one code chip surface area, there is small effect on either signal power or correlation (Λ function) smearing, and the ionospheric delay determination retains accuracy.

On the other hand, if the glistening surface lies outside one code chip delay surface area, then the signal power must decline and the smearing must increase. Thus, the accuracy of the ionospheric range error must decrease.

Another point to remember is that the ocean bounce signal must be almost exclusively left-hand circularly polarized for higher grazing angles. A left-hand polarized antenna is then necessary. At lower grazing angles, the signal becomes elliptically polarized and it may be possible or even desirable to use both the right- or left-hand or both polarization components.

The apparent time delay may be incorrect and lead to processing errors. Since the code phase ambiguity range is 300 km, it is possible to have a bounce at satellite altitudes appear earlier or later than the direct signal. The possibility results of having the delay signal appear as if the bounce path is closer than the direct signal.

In summary, it appears that the GPS bounce signal from the ocean can, under certain circumstances, be used to determine the ionospheric TEC in the satellite vicinity. Determining the TEC and applying the results to ionosphere models could extend their accuracy over areas where such improvement is greatly needed.

NASA Langley Research Center
Hampton, VA 23681-0001
October 16, 1996

Appendix

Signal Power Structure

To form the connection between equation (19) in this report and its development in reference 2, it is necessary to start with equation (3) from section 3.1 of reference 2 as follows:

$$E = \exp(i\omega t - ik.r) \quad (\text{A1})$$

and notice that the spread spectrum signal from a GPS satellite can be modelled as a modulation $a(t)$ multiplied by the monochromatic field as follows:

$$E = a(t) \exp(i\omega t - ik.r) \quad (\text{A2})$$

which yields the correct real part. For the C/A code of a GPS satellite, the modulation $a(t)$ is much slower than the carrier frequency and consequently E can be thought of as monochromatic, with a DC amplitude in all cases except the cross-correlation. Equation (8) and succeeding equations from reference 2 will be unaltered. The reflected electric field can be expressed by using equations (32) and (33) from section 3.1 of reference 2 as follows:

$$E_2 = \frac{ik \exp(ikR_0)L \cos\theta_1}{\pi R_0} \int_{-L}^L \frac{(a\zeta' - b) \exp(iv_x x + iv_z \zeta) dx}{4L \cos\theta_1} \quad (\text{A3})$$

or including the time dependence with the modulation term:

$$E_2 = \frac{ik \exp(ikR_0)L \cos\theta_1}{\pi R_0} \int_{-L}^L \left[\frac{a\zeta' - b \exp(iv_x x + iv_z \zeta) dx}{4L \cos\theta_1} \right] a(t) \exp(i\omega t - ik.r) \quad (\text{A4})$$

Equation (A4) must be modified to include the two-dimensional version not explicitly stated in reference 2. The dimension L becomes X and Y . Noting that the dimensions X and Y are only one half the side of the reference area and ignoring the time dependence momentarily, the scattered field is

$$E_2 = \frac{ik \exp(ikR_0)XY \cos\theta_1}{\pi R_0} \int_X^X \int_{-Y}^Y \frac{(a\zeta'_x + c\zeta'_y - b) \exp(iv_x x + iv_y y + iv_z \zeta) dy dx}{4XY \cos\theta_1} \quad (\text{A5})$$

The first term can be related to the reflected field along the specular point as follows:

$$E_{20} = \frac{ik \exp(ikR_0)XY \cos\theta_1}{\pi R_0} \quad (\text{A6})$$

Dividing equation (A5) by equation (A6) gives the scattering coefficient r of equation (1), section 3.2 (ref. 2), as

$$E_2 = \frac{1}{2} E_{20} \int_{-X}^X \int_{-Y}^Y \left[\frac{(a\zeta'_x + c\zeta'_y - b) \exp(iv_x x + iv_y y + iv_z \zeta) dy dx}{4XY \cos\theta_1} \right] \quad (\text{A7})$$

where the factor $1/2$ is different from equation (9) of section 3.2 (ref. 2) and represents what may be an error in equation (9) stemming from the evaluation of the unit reflectivity case and dropping the factor of 2 common to each factor in equations (6) – (8) of section 3.2 (ref. 2). If the constant outside the integrals in equation (9) (ref. 2) is multiplied by a factor of 2, the excess factor of $1/2$ will cancel. The rest of the development leading to equation (11) of section 3.2 (ref. 2) is then brought into agreement. The formula for ρ can then be identified as the factors in the integrals as follows:

$$E_2 = E_{20} \rho \quad (\text{A8})$$

Assuming that the detected signal in the code correlation receiver is proportional to the electric field strength (proportionality constant equal unity) allows retention of the geometric, stochastic, and reflectivity effects. The equation relating the short time average of the cross-correlation can then be written as

$$\begin{aligned} \langle y^2(\tau) \rangle &= \frac{A^2 \cos^2 \theta_1}{\lambda^2 R_0^2} \iint \Lambda^2 \left(\tau - T_{as} - \frac{\delta}{c} - t_{\text{off}} \right) F_3^2 \exp[i\nu_x(x-x') + i\nu_y(y-y')] \\ &\quad \times \frac{\langle \exp[i\nu_z(\zeta - \zeta')] \rangle d^2 r_s d^2 r'_s}{A^2 \cos^2 \theta_1} \end{aligned} \quad (\text{A9})$$

The function Λ^2 represents the correlation processing in the receiver with scale factors taking into account the conversion efficiency of the receiver for the detected electric field. Assuming that the surface correlations occur over (effectively independent) areas considerably smaller than the C/A code chip dimension, the Λ^2 term can be removed from the expectation as follows:

$$\langle y^2(\tau) \rangle = \frac{A^2 \cos^2 \theta_1}{\lambda^2 R_0^2} \langle \rho \rho^* \rangle \Lambda^2 \left(\tau - T_{as} - \frac{\delta}{c} - t_{\text{off}} \right) \quad (\text{A10})$$

where $\langle \rho \rho^* \rangle$ is given by

$$\langle \rho \rho^* \rangle = \frac{F_3^2 \lambda^2 \cot^2 \beta_0 \exp(-\tan^2 \beta / \tan^2 \beta_0)}{A \pi (\cos \theta_1 + \cos \theta_2)^2} \quad (\text{A11})$$

Note that in reference 2, the expectation yields another factor of A and when taken with the first factor of A^2 in equation (A9), equation (A9) is left linear in area.

Moving to the differential in scattering area ($A \rightarrow dA$), $\langle y^2(\tau) \rangle$ can be identified as directly proportional to received power per unit area scattered per power per unit area of incoming radiation. The second factor in equation (A10) can be identified with equation (62), section 5.3 of reference 2.

Incorporating the simplifications leading to equation (7) in reference 2, section 12.4.1, the total signal after squaring and as a function of τ can be obtained by integrating over the area of the surface being illuminated and within the glistening surface as follows:

$$\begin{aligned} \int \langle y^2(\tau) \rangle d^2 r &= \int \left[\cot^2 \beta_0 \exp(-\tan^2 \beta / \tan^2 \beta_0) \right. \\ &\quad \left. \times \Lambda^2 \left(\tau - T_{as} - \frac{\delta}{c} - t_{\text{off}} \right) \right] \frac{d^2 r}{\pi R_0^2} \end{aligned} \quad (\text{A12})$$

Under the conditions that the integral can be evaluated over contours of constant δ , the Λ^2 integration can be identified as a convolution of the Λ^2 function with another function of δ arising from the appropriate surface areas.

References

1. Auber, Jean-Claude; Bibaut, Alain; and Rigal, Jean-Marie: Characterization of Multipath on Land and Sea at GPS Frequencies. *Proceedings of 7th International Technical Meeting of the Satellite Division of the Institute of Navigation*, Part 2, *ION GPS-94*, Sept. 1994, pp. 1155–1171.
2. Beckmann, Petr; and Spizzichino, André: *The Scattering of Electromagnetic Waves From Rough Surfaces*. Artech House, Inc., 1987.
3. Parkinson, Bradford W.; and Spilker, James J., Jr. eds: *The Global Positioning System—Theory and Application*. AIAA, 1995.
4. Papagiannis, Michael D.: *Space Physics and Space Astronomy*. Gordon and Breach Sci. Publ., 1972.

REPORT DOCUMENTATION PAGE

Form Approved
OMB No. 0704-0188

Public reporting burden for this collection of information is estimated to average 1 hour per response, including the time for reviewing instructions, searching existing data sources, gathering and maintaining the data needed, and completing and reviewing the collection of information. Send comments regarding this burden estimate or any other aspect of this collection of information, including suggestions for reducing this burden, to Washington Headquarters Services, Directorate for Information Operations and Reports, 1215 Jefferson Davis Highway, Suite 1204, Arlington, VA 22202-4302, and to the Office of Management and Budget, Paperwork Reduction Project (0704-0188), Washington, DC 20503.

1. AGENCY USE ONLY <i>(Leave blank)</i>	2. REPORT DATE December 1996	3. REPORT TYPE AND DATES COVERED Technical Memorandum	
4. TITLE AND SUBTITLE Utilizing GPS To Determine Ionospheric Delay Over the Ocean		5. FUNDING NUMBERS WU 225-99-00-01	
6. AUTHOR(S) Stephen J. Katzberg and James L. Garrison, Jr.			
7. PERFORMING ORGANIZATION NAME(S) AND ADDRESS(ES) NASA Langley Research Center Hampton, VA 23681-0001		8. PERFORMING ORGANIZATION REPORT NUMBER L-17575	
9. SPONSORING/MONITORING AGENCY NAME(S) AND ADDRESS(ES) National Aeronautics and Space Administration Washington, DC 20546-0001		10. SPONSORING/MONITORING AGENCY REPORT NUMBER NASA TM-4750	
11. SUPPLEMENTARY NOTES			
12a. DISTRIBUTION/AVAILABILITY STATEMENT Subject Category 43 Unclassified-Unlimited Availability: NASA CASI (301) 621-0390		12b. DISTRIBUTION CODE	
13. ABSTRACT <i>(Maximum 200 words)</i> Several spaceborne altimeters have been built and flown, and others are being developed to provide measurements of ocean and ice sheet topography. Until the launch of TOPEX, altimeters were single frequency systems incapable of removing the effects of ionospheric delay on the radar pulse. With the current state of the art in satellite altimetry, the ionosphere causes the largest single error when using single frequency altimeters. Ionospheric models provide the only recourse short of adding a second frequency to the altimeter. Unfortunately, measurements of the ionosphere are lacking over the oceans or ice sheets where they are most needed. A possible solution to the lack of data density may result from an expanded use of the Global Positioning System (GPS). This paper discusses how the reflection of the GPS signal from the ocean can be used to extend ionospheric measurements by simply adding a GPS receiver and downward-pointing antenna to satellites carrying single frequency altimeters. This paper presents results of a study assessing the feasibility and effectiveness of adding a GPS receiver and downward-pointing antenna to satellites carrying single frequency altimeters.			
14. SUBJECT TERMS GPS; GPS multipath; Ionosphere correction; Altimeter; Satellite; Models		15. NUMBER OF PAGES 14	
		16. PRICE CODE A03	
17. SECURITY CLASSIFICATION OF REPORT Unclassified	18. SECURITY CLASSIFICATION OF THIS PAGE Unclassified	19. SECURITY CLASSIFICATION OF ABSTRACT Unclassified	20. LIMITATION OF ABSTRACT